NeuroImage 270 (2023) 119942

Contents lists available at ScienceDirect

NeuroImage

journal homepage: www.elsevier.com/locate/neuroimage

Hierarchical psychophysiological pathways subtend perceptual asymmetries in Neglect

Francesco Di Gregorio[a], Valeria Petrone[b], Emanuela Casanova[b], Giada Lullini[b], Vincenzo Romei[c], Roberto Piperno[b], Fabio La Porta[b,*]

[a] UOC Medicina Riabilitativa e Neuroriabilitazione, Azienda Unità Sanitaria Locale, Bologna 40133, Italy
[b] IRCCS Istituto delle Scienze Neurologiche di Bologna, Bologna, Italy
[c] Dipartimento di Psicologia, Centro Studi E Ricerche in Neuroscienze Cognitive, Alma Mater Studiorum – Università di Bologna, Campus di Cesena, Cesena 47521, Italy

ARTICLE INFO

Keywords:
EEG
Left hemispatial neglect
Stroke
Structural Equation Modeling
Visuospatial perception

ABSTRACT

Stroke patients with left Hemispatial Neglect (LHN) show deficits in perceiving left contralesional stimuli with biased visuospatial perception towards the right hemifield. However, very little is known about the functional organization of the visuospatial perceptual neural network and how this can account for the profound reorganization of space representation in LHN.

In the present work, we aimed at (1) identifying EEG measures that discriminate LHN patients against controls and (2) devise a causative neurophysiological model between the discriminative EEG measures. To these aims, EEG was recorded during exposure to lateralized visual stimuli which allowed for pre-and post-stimulus activity investigation across three groups: LHN patients, lesioned controls, and healthy individuals. Moreover, all participants performed a standard behavioral test assessing the perceptual asymmetry index in detecting lateralized stimuli. The between-groups discriminative EEG patterns were entered into a Structural Equation Model for the identification of causative hierarchical associations (i.e., pathways) between EEG measures and the perceptual asymmetry index.

The model identified two pathways. A first pathway showed that the combined contribution of pre-stimulus frontoparietal connectivity and individual-alpha-frequency predicts post-stimulus processing, as measured by visual-evoked N100, which, in turn, predicts the perceptual asymmetry index. A second pathway directly links the inter-hemispheric distribution of alpha-amplitude with the perceptual asymmetry index. The two pathways can collectively explain 83.1% of the variance in the perceptual asymmetry index.

Using causative modeling, the present study identified how psychophysiological correlates of visuospatial perception are organized and predict the degree of behavioral asymmetry in LHN patients and controls.

1. Introduction

Left Hemispatial Neglect (LHN) is a frequent and disabling neuropsychological syndrome associated with deficits in perceiving, responding, and orienting attention toward the contralesional hemifield (Bartolomeo et al., 2007; Ladavas et al., 1987; Parton et al., 2004). LHN is often due to right hemispheric stroke with lesions over the frontoparietal brain network (FPN, (Bartolomeo et al., 2012, 2007). These lesions cause abnormal functioning over the dorsal (DAN) and ventral attention networks (VAN, Corbetta et al., 2005; Mort et al., 2003). These networks are right hemisphere dominant and while the DAN is involved in orienting perceptual resources toward relevant spatial locations (the "*where*" pathway, Capotosto et al., 2009; Husain and Nachev, 2007; Thiebaut de Schotten et al., 2011), the VAN has been described as the "*what*" pathway (Parr and Friston, 2018; Ungerleider, and Haxby, 1994), propagating perceptual information about stimulus identity.

Many studies and computational models suggest that the functional integrity of the FPN and the connectivity between the areas of this network subtend visuospatial perception (Bartolomeo et al., 2007; Briggs et al., 2013; Corbetta and Shulman, 2002; Doricchi et al.,

* Corresponding author.
E-mail addresses: fabiolaporta@mail.com, fabio.laporta@isnb.it (F. La Porta).

https://doi.org/10.1016/j.neuroimage.2023.119942.
Received 10 October 2022; Received in revised form 25 January 2023; Accepted 13 February 2023
Available online 14 February 2023.

2008; He et al., 2007, 2007; Hembrook Short et al., 2017; Hembrook-Short et al., 2019; Parr and Friston, 2018). Within this system, neuroimaging studies suggest that LHN involves imbalances in the activity of the two hemispheres and low inter-hemispheric connectivity (Bartolomeo, 2021; Bartolomeo et al., 2012; Carter et al., 2010; Dambeck et al., 2006). In particular, fMRI studies identified over-activations of the intact left hemisphere in LHN (Corbetta et al., 2005). This over-activation can bias attention towards the contralateral hemifield, leading to perceptual asymmetries. This evidence is further supported by a recent EEG study showing abnormal anticipatory pre-stimulus alpha distribution in LHN with larger amplitude over the left hemisphere compared to the right (Lasaponara et al., 2019). The inter-hemispheric imbalance is supposed to be the neural substrate of the lateralization of perceptual dysfunctions and is considered an important biomarker of LHN. Accordingly, several neurostimulation protocols have been applied to reduce inter-hemispheric imbalance in LHN and results are promising in terms of the reduction of the perceptual bias towards the right hemifield (Brighina et al., 2003; Jacquin-Courtois, 2015; Koch et al., 2012; Oliveri, 2011).

Notably, the speed of alpha oscillations also plays a crucial role in the perceptual processing of incoming sensory stimuli with faster alpha oscillations leading to higher perceptual sampling and more accurate perceptual experience (Bertaccini et al., 2022; Cecere et al., 2015; Coldea et al., 2022; Cooke et al., 2019; Di Gregorio et al., 2022c; Samaha and Postle, 2015; Trajkovic et al., 2022). In particular, faster pre-stimulus Individual Alpha Frequency (IAF), which is the frequency peak within the alpha band, predicts better perceptual accuracy (Di Gregorio et al., 2022c; Trajkovic et al., 2022). Moreover, alpha-frequency is commonly impaired after stroke, with peaks shifting over slower frequencies (Pietrelli et al., 2019; Qureshi et al., 2018), leading to various perceptual and cognitive impairments(Giaquinto et al., 1994; Ippolito et al., 2022; Qureshi et al., 2018). In general, dysfunctions of the FPN and pre-stimulus alpha activity might be considered the neural basis of perceptual asymmetries and deficits in LHN (Corbetta et al., 2005; Husain and Rorden, 2003). Furthermore, besides alterations at the anticipatory pre-stimulus level, there is also evidence of impaired stimulus processing. In particular, LHN patients show an impaired amplitude and delayed latency in the visual-evoked N100 and P300 in response to the right presented stimuli (Deouell et al., 2000; Di Russo et al., 2008; Doricchi et al., 2021; Lasaponara et al., 2021; Verleger et al., 1996).

The Pre- and post-stimulus EEG measures are widely used to investigate neural substrates of multiple stages of perception in healthy participants and to characterize perceptual deficits in LHN patients (Lasaponara et al., 2021). However, although EEG measures can reflect essential aspects of perceptual processing, single measures may not be able to capture the complexity of visuospatial perception. For instance, it is unclear how EEG measures are associated with each other and how the underlying psychophysiological networks and pathways are organized in the healthy brain and LHN. Thus, we hypothesized that different pre- and post-stimulus EEG parameters, known to subtend visuospatial perception based on the current literature, can be associated and organized in hierarchical networks.

To test these hypotheses, we set the following two aims: (1) To *identify EEG measures that discriminate patients with LHN against controls.* We presented to a sample of LHN patients, healthy and brain damaged controls (i.e., patients with no evidence of LHN) lateralized visual stimuli during EEG recording to extract EEG correlates of visuospatial perception. Then, EEG correlates were compared between the three groups to identify those EEG measures best discriminating LHN from controls. (2) To *devise a causative neurophysiological model between EEG measures*. To reach this aim, we applied Structural Equation Models (Bentler and Yuan, 1999; Hair et al., 2014; Koechlin et al., 2003) (i.e., SEM) to define the causative associations and hierarchies between the EEG measures identified in the first step and to study whether and to what extent EEG measures can collectively predict perceptual performance measured by the perceptual asymmetry index (Mancuso et al., 2019).

2. Materials and methods

2.1. Aim 1: To identify EEG measures that discriminate patients with LHN against controls

2.1.1. Population

For this aim, we planned to enroll three groups of patients. The first group (Left Hemispatial Neglect, LHN) included stroke patients with clinical evidence of left hemispatial neglect assessed with the Bells Test (inclusion criterion for LHN patients = asymmetry score in the Bells test > 3) (Mancuso et al., 2019). The second group (Brain Damaged Control, BDC) included stroke patients with no clinical evidence of left hemispatial neglect (inclusion criterion = asymmetry score in the Bells test < 3). Eligibility criteria for all stroke patients were: 1. Diagnosis of ischemic or hemorrhagic stroke confirmed by encephalic CT scan or MRI; 2. Inpatient or outpatient rehabilitation setting; 3. Age between 18 and 80 years; 4. Time after stroke between 3 weeks and 12 weeks; 5. Adequate language comprehension to give informed consent. Exclusion criteria: 1. Medical instability at the time of enrollment; 3. Presence of alteration in the consciousness-vigilance rhythm; 4. Cortical blindness, visual agnosia and/or evidence of hemianopia reporting occipital lesions; 5. Previous psychiatric disorders and/or history of substance abuse; 6. Severe reduction of visual acuity not compensated by optic lenses; and 7. previous diagnosis of cognitive impairment. All patients, after enrollment, performed a broader assessment of Neglect related symptoms (i.e., the Fluff Test and the Picture Scanning test) and of the motor functioning (i.e., the Motricity index in the right limbs, MI). BDC patients showing Neglect related symptoms during the assessment were not included in the study. The third group included voluntary healthy participants (Healthy Controls, HC). All participants were recruited at *UOC Medicina Riabilitativa e Neuroriabilitazione* of the IRCCS Istituto delle Scienze Neurologiche di Bologna, Italy. Participants gave written informed consent before participating in the study, and all procedures were conducted in accordance with the Declaration of Helsinki and approved by the Ethical Committee Area Vasta Emilia Centro (CE num. 17075) Bologna, Italy.

2.1.2. Intervention: experimental procedure 1

All participants underwent EEG recordings. During the experimental sessions, participants were comfortably seated in a silent room with dimmed light and requested to attend the presentation of lateralized visual stimuli (Fig. 1A) during concurrent EEG recordings. No active action was requested in response to the stimulus presentation. The stimulus presentation protocol was programmed in a PC running the “Presentation” software (Neurobehavioral Systems, Albany, CA), which, during EEG recording, controlled stimuli presentation. Stimuli were presented on a 21-inch color monitor, and participants kept a constant viewing distance of 50 cm. Each trial started with a white central fixation cross over a black background, and participants were prompted to fix the central fixation cross throughout the experiment. Then, after a varying stimulus onset asynchrony (SOA between 640 and 960 ms with steps of 80 ms), a stimulus was presented randomly on the right or the left of the fixation cross along the midline on a view distance angle of 28°. Stimuli were yellow squares (1 cm X 1 cm) presented in the black background to optimize color contrast between the stimulus and the background. Stimuli were displayed for 96 ms; the central fixation cross was kept on the screen for 1000 ms before the beginning of the subsequent trial. An expert technician visually monitored eye movements and whenever participants lost the central fixation provided feedbacks to recover it. Sixty-four stimuli were presented in a single block (32 in each hemifield).

EEG data were recorded using the BrainVision recorder system from 19 Ag/AgCl-cup electrodes positioned according to the 10/20 system and referenced to the linked ear lobes. The EEG signal was recorded from 12 scalp electrodes: Fz, Cz, Pz, C4, C3, P4, P3, F4, F3, Oz, O1, O2. The CMS Common Mode Sense (CMS) and the Driven Right Leg (DRL) electrodes were used as reference and ground electrodes. Impedance

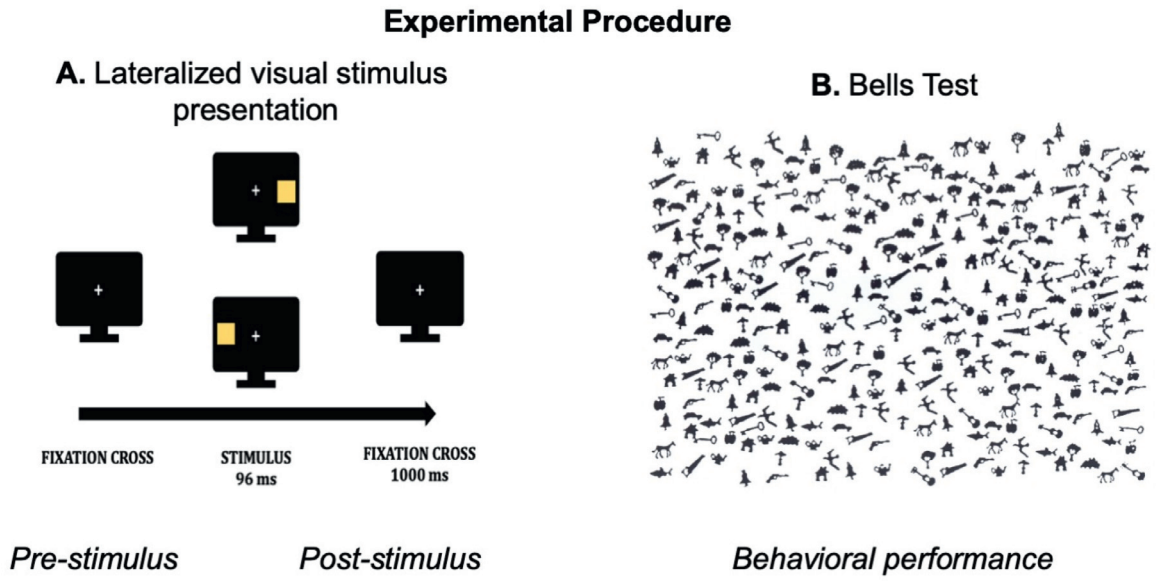

Fig. 1. Experimental procedure. A. Lateralized visual stimulus presentation. In the pre-stimulus time, a fixation cross is presented on a black background for 1 s. Then, a stimulus is presented randomly for 96 milliseconds (ms) either on the left or right of the fixation cross. Before a new trial begins, the fixation cross is again presented for 1 sec (post-stimulus time period). **B**. Bells Test protocol. After each EEG session, participants were asked to cross out all the bells on a A4 paper and ignore the other figures to study clinical and behavioral performance.

for EEG and electrooculogram (EOG) electrodes were kept below 10 kΩ. The vertical and horizontal electrooculogram (EOG) was recorded from electrodes above and below the right eye and on the outer canthi of both eyes. EEG and EOG data were continuously recorded at a sampling rate of 1024 Hz (Babiloni et al., 2020). Offline, all electrodes were re-referenced to the average reference, re-sampled to 500 Hz, and filtered with a 0.5–30 Hz band-pass filter. EEG data were analyzed using EEGLAB v14.0.0 (Delorme and Makeig, 2004) and custom routines written in MatLab R2015b (The Mathworks, Natick, MA, USA). For the stimulus-locked data, epochs of 1000 ms before and 1000 ms after stimulus onset were extracted and baseline-corrected using the entire pre-stimulus period. Epochs contaminated with artifacts were excluded using the pop_autorej function in EEGLAB v14.0.0, which first excludes trials with voltage fluctuations higher than 1000 μV and then excludes trials with data values outside five standard deviations using an iterative algorithm. The mean percentage of excluded trials was 14.45% (SE = 1.17%) for the stimulus-locked averages (excluded trials in the LHN = 17.7%, SE = 2.53%; BDC = 12.46%, SE =1.48%; HC = 12.46%, SE =1.23%). No statistically significant differences emerged in the percentage of excluded trials between groups ($F(2,36) = 2.55$; $p = .093$). Three EEGs were excluded from the analyses for abundant artifacts. An independent components analysis (ICA) was performed for each participant's EEG (Jutten and Herault, 1991; Makeig et al., 1996) using the infomax algorithm (Bell and Sejnowski, 1995) to correct the remaining artifacts. Then, independent components (ICs) representing stereotyped artifact activity, such as horizontal (saccades) and vertical (blinks) eye movements, and muscle artifacts were identified through a multistep correlational template-matching process implemented in CORRMAP v1.02 (Campos Viola et al., 2009). Topographies of ICs labeled as artifacts by the CORRMAP procedure were visually inspected and then calculated out of the data using inverse matrix multiplication. Artifact corrected epochs were categorized based on stimulus location in left and right trials.

The overall experimental procedure duration was about 20 min. Participants repeated the procedure and the EEG recording during four consecutive days (2 participants repeated the EEG 8 times) for a total of 154 EEG recordings. Each EEG recording was used as a separate session in the analyses. The EEG experimental design was already presented in previous studies (Di Gregorio et al., 2021a, 2021b).

2.1.3. Control

No control for the intervention was planned, but BDC and HC groups were used as control groups.

2.1.4. Outcome

Measures based on EEG data (i.e., EEG features), known to be associated to visuospatial perception, were extracted before and after stimulus presentation, establishing a temporal hierarchy between EEG features. Thus, we distinguished three main outcome measures: EEG features preceding (i.e., pre-stimulus features) and following stimulus presentation (i.e., post-stimulus processing) and a behavioral performance test.

1 **Pre-stimulus features**. Alpha parameters (IAF and alpha-amplitude) and connectivity measures (phase lag index) were extracted from the pre-stimulus activity. IAF and alpha-amplitude were computed from the power spectra of each EEG session. To identify the IAF, data epochs in the 1000 ms following the presentation of the fixation cross (i.e., pre-stimulus alpha from -1000 ms to stimulus presentations) were analyzed with a fast Fourier transformation (MatLab function spectopo, frequency resolution: 0.166 Hz). Power was calculated in this time window and normalized in (10*log10(μv)2) at each frequency. IAF was defined as the maximum local power within 7-13 Hz (i.e., alpha range). In the same time window, alpha-amplitude was defined as the maximum alpha power, expressed in normalized power. IAF and alpha-amplitude were measured over frontal (electrodes F3 and F4), parietal (electrodes P3 and P4) and occipital (electrodes O1 and O2) regions of interest (ROIs) in the right and left hemispheres. To calculate the phase lag index (PLI) (Stam et al., 2007; Vinck et al., 2011), pre-stimulus EEG data were merged into 1000 ms non-overlapping windows (Lee et al., 2019; Trajkovic et al., 2021). Then the cross-spectra of the time series signals were calculated, where PLI estimates the magnitude of the imaginary part of the cross-spectrum between pairs of electrodes. Specifically, the PLI calculates phase differences (i.e., phase lag) between two time series signals and can assume values between 0 and 1. Larger PLI values reflect a consistent phase lag between two signals. If the relation between two signals is random or the phases coincide (as for electrodes with same neural source), the PLI value is 0. Moreover, a threshold for each participant is set to detect residual false positive

connectivity. For this reason, The PLI is a robust estimator of scalp-level connectivity that is more invariant to volume conduction in comparison to other estimators (Hardmeier et al., 2014; Stam et al., 2007). For each EEG, PLI was estimated as a function of individual alpha frequency peaks (for methods details see also (Di Gregorio et al., 2022a; Trajkovic et al., 2021), and 12 × 12 connectivity matrices were generated over the scalp electrodes. Inter-hemispheric connectivity based on PLI was estimated between parietal (PLI between P3-P4) and frontal (PLI between F3-F4) electrodes, while frontoparietal connectivity was estimated in the right (PLI between F4-P4) and the left hemisphere (PLI between F3-P3).

2 **Post-stimulus features.** Visual-evoked potentials (VEPs) in the post-stimulus time window (i.e., from stimulus presentations to 1000 ms after) were calculated. The amplitude in microvolt (μv), and the latency in milliseconds (ms) of the negative peak of the N100 (time window between 80 ms and 200 ms) were analyzed separately for left and right-presented stimuli over parietal electrodes (i.e., P3 and P4) (Di Gregorio et al., 2021a, 2021b; Di Russo et al., 2013, 2008). Then, indices based on VEPs were extracted. In particular, the Visuospatial Attention Bias Index (vABI) (Di Gregorio et al., 2021a, 2021b) was calculated on the N100 peak amplitude, and the Inter-Hemispheric Transmission Time (IHTT) (Moes et al., 2007), was calculated on the N100 peak latency. The vABI is a lateralization index which reflects the difference in the activation of the two hemispheres in response to lateralized stimuli. Specifically, positive values of the vABI reflect larger activations for right presented stimuli and thus a right bias in visual processing, while negative values reflect a left bias. Details of vABI calculation are reported in previous studies (Di Gregorio et al., 2021a, 2021b). Similarly, the IHTT reflects the transmission times of lateralized information between the two hemispheres (from right to left and from left to right hemispheres (Brown et al., 1994; Moes et al., 2007). In particular, the right to left IHTT (r-l IHTT) is calculated as the difference between the latencies of the negative peak of N100 for left presented stimuli over electrodes P4 and P3 (i.e., r-l IHTT = N100 latency over P4 – N100 latency over P3). Instead, the left to right IHHT (l-r IHTT) is calculated for right presented stimuli as the difference: N100 latency over P3 – N100 latency over P4. The same indexes (i.e, the vABI and the IHTT) with the same procedures were also calculated for the P300 in a time window between 200-400 ms relative to stimulus onset.

3 **Behavioral performance test**. After each EEG session, all participants underwent a Bells Test (Mancuso et al., 2019) (Fig. 1B) to assess asymmetries in lateralized perception. Asymmetry scores were calculated as the difference between the number of target bells checked on the right and the left side. Positive values indicate a more considerable number of misses on the left side, indicating asymmetries in spatial perception (Mancuso et al., 2019).

2.1.5. Statistical analyses

To reach the first aim, we compared EEG features across EEG sessions between groups (HC, BDC, and LHN) to identify neural correlates, which could discriminate between individuals without (healthy participants and brain damaged controls) and with left hemispatial neglect. The variables Age and Gender were included as additional covariates in the analyses for all the EEG measures. Between-subjects planned comparisons were analyzed using two-tailed independent samples t-tests (for all measures) and two-way mixed-model ANCOVAs with repeated measurements (for IAF, alpha amplitude and connectivity). The within-subject variable ROI for IAF and alpha-amplitude was calculated over electrodes (O1, O2, P3, P4, F3, and F4) and for PLI connectivity over electrodes pairs (P3-P4, F3-F4, F3-P3 and F4-P4), while IHTT was analyzed for the within-subject variable direction (right to the left and left to right). One-way ANCOVAs were used to analyze the vABI and the clinical data between groups. The significance level was set at $p < .05$. Greenhouse-Geisser correction was applied when necessary (Greenhouse and Geisser, 1959) to compensate violations of sphericity. 1000 Bootstrap correction was applied whenever necessary for multiple comparisons. Effect sizes were reported as Cohen's d (d) for the t-test and partial eta squared (ηp^2) for the ANCOVAs. All analyses were performed with MatLab and SPSS software (version 13).

2.2. Aim 2: To devise a causative neurophysiological model between EEG measures

To reach this aim, we built a hierarchical causative model with structural equation modelling (SEM) techniques based on the data generated within aim 1. The experimental procedure used in aim 1 (i.e., EEG and behavioral performance assessed with an external test, the Bells Test) is particularly indicated for SEM applications. Indeed, the SEM analyzes the causative relationship between latent variables (Tenenhaus et al., 2005; Vinzi et al., 2010) and models single variables or their associations (i.e., pathways) to predict external clinical outcomes. A crucial advantage of SEM is that the model can identify associations between different types of measures (i.e., psychophysiological and behavioral measures) and can provide a statistical-driven approach, based on the hypothesis (i.e., confirmatory analysis), describing the structure underlying the observed variables. In other words, the SEM model can link the functioning of psychophysiological networks with the behavioral performance in external clinical tests. SEM models have been previously implemented in experimental and clinical neurosciences to investigate cognitive functioning in healthy participants (Koechlin et al., 2003) and to predict behavioral and clinical outcomes in neurological and psychiatric patients (Koshiyama et al., 2021; Parkes et al., 2019; Wang et al., 2019, p. 201)

2.2.1. Model generation

To build the model, we hypothesized the following latent variables:

1 First-order variables (pre-stimulus time period): perceptual sampling (IAF over the ROIs as indicators), attention distribution (alpha-amplitude over the ROIs as indicators) and connectivity within the visuospatial perceptual network (PLI over the ROIs as indicators).
2 Second-order variables (post-stimulus time period): stimulus processing bias (vABI as single indicator) and latency (right to left and left to right IHTT as indicators).
3 Higher order variable (behavioral performance): perceptual asymmetry, indicated by the asymmetry score generated by the Bells test.

Based on the literature data, we hypothesized an initial model, where all first-order latent variables influenced both the second-order and the higher order latent variable, assuming that the latter was also influenced by the second-order latent variables. In other words, the initial model was conceived to be able to capture all possible connections and the temporal progression of perceptual processing, distinguishing earlier pre-stimulus and later post-stimulus EEG activity as well as behavioral performance.

Based on the results generated from aim 1, the best between-groups discriminative EEG features were associated to the corresponding hypothesized latent variable (Koshiyama et al., 2021). In this way, the initial hypothesized model was completed by associating a specific observable indicator (EEG feature) to each first- and second-order latent variable. Preliminary Shapiro-Wilk test for normality distribution was performed for all measures (Shapiro and Wilk, 1965).

2.2.2. Model assessment

SEM analyses were performed with Partial Least Squares using the PLS-PM MatLab toolbox (Aria et al., 2018). The overall model assessment was performed using the following fit statistics: χ^2, RMSEA (Root Mean Square Error of Approximation), SRMR (Standardized Root Mean Square Residual), CFI (Comparative Fit Index) and TLI (Tucker-Lewis Index) (Xia and Yang, 2019). Fit to the model was considered adequate if the χ^2 was not significant, RMSEA <.06, SRMS< .08 CFI >.90, TLI>.95(Aria et al., 2018). SRMR is particularly indicated for studies

with sample sizes < 500 units (Cangur and Ercan, 2015). However, the primary indicator of model fit is the χ^2 statistic, which provides a test for the null hypothesis that the theoretical model does not fit the data. Models with non-significant χ^2 statistics are deemed to have good fit. Root Mean Square Error of Approximation (RMSEA) is a measure of model fit relatively unaffected by sample size and model estimation methods. The Comparative fit index (CFI) compares the model with a null model, which assumes that the main variables in the model are not associated (i.e., the independence model). The Tucker-Lewis Index (TLI) is an incremental fit index which is not significantly affected by sample sizes. Larger TLI value indicates better fit for the model but 0.95 is reported in the literature as an acceptable cut-off value (Cangur and Ercan, 2015; Gibbons et al., 2013). Internal consistency of the model (i.e., construct reliability) was assessed for each variable with the Cronbach Alpha. Construct reliability was considered adequate for between groups analyses or for single subject analyses with Cronbach Alpha > .70 or >.85 respectively (Pellicciari et al., 2020).

Loadings were calculated for each variable to analyze the reliability of single indicators, and loadings less than 0.4 were excluded (Aria et al., 2018). Convergence validity, which calculates if a set of indicators represents only one underlying latent variable, was expressed in Average Variability Explained (AVE). Convergence Validity is satisfied if AVE > .50. A path-weighting scheme specifies the relationships between latent variables, and total effects (i.e., path coefficients) are reported. Path coefficients were bias-corrected (500 Bootstrap replications). p-values and 95% confidence intervals are reported.

2.2.3. Model identification and sample size estimation

An overidentified model is a model that is based on enough information in the data to estimate the model parameters (i.e., the number of estimable parameters is less than the number of data points, such as variances and covariances of the observed variables). This situation results in positive degrees of freedom that allow for scientific use of the model (Byrne, 2011). Degrees of freedom (df) are calculated with the following formula 1:

$$df = p(p+1)/2$$

where p is the number of estimated model parameters (6 in the final model). Thus, accordingly to the formula 1, degrees of freedom for our model are 21, which identifies the model as overidentified. Raykov and Marcoulides (2006) recommended a minimum sample size greater than 10 times the number of estimated model parameters for SEM analyses. As in our model estimated parameters are 6, the minimum sample size would be 60. The sample size used in our model (151 EEG sessions) was larger of the minimum requested.

2.3. Data and code availability statement

The clinical datasets used and analyzed during the current study are available from the corresponding author on request. The anonymized EEG raw data are publicly available for download at zenodo.org.

3. Results

3.1. Aim 1: To identify EEG measures that discriminate patients with LHN against controls

For aim 1, 37 participants were enrolled. Of these, 14 patients suffered of right hemispheric stroke and presented clinical evidence of left hemispatial neglect (LHN group), while 9 patients had no clinical evidence of left hemispatial neglect (BDC group). 14 healthy participants (7 females, age mean = 49.3, SE = 3.23) were additionally included as control group (HC group). Demographic data and lesion profiles are reported in Table 1. No lesion size analyses were reported. In fact, lesion data were collected from MRI or TC (see inclusion criteria), thus we cannot provide a coherent measure of the lesion size for all patients. The two stroke patient groups (LHN and BDC) did not significantly differ in the initial level of stroke severity, as demonstrated by the National Institute of Health Stroke Scale (NIHSS) score ($t(21)=0.2$, $p=.984$, $d=0.041$), or in the time elapsed from stroke to enrollment (LHN = 30.57 days, SE = 3.39; BDC = 34.55 days, SE = 4.44) ($t(21)=0.72$, $p=.479$, $d=0.099$). Moreover, BDC group was screened to exclude visuo-spatial deficit. To this aim, we used a standardized neuropsychological test battery assessing selective attention (Attentional Matrices) and visuospatial short-term memory (Digit and Corsi Span). The patients' performance was compared to large sample normative data, in which raw scores are first adjusted for age, sex, and education, and then transformed into stan-

Table 1
Demographic and clinical data.

Patients (Case)	*Group (LHN,BDC)*	*Sex (M/F)*	*Age (years)*	*Lesion Location (Areas)*	*NIHSS (Score)*
1	LHN	M	59	rPPC, rFPC, rTha	19
2	LHN	M	54	rPPC, rFPC	8
3	LHN	F	53	rPPC	15
4	LHN	M	66	rPPC, rFPC	21
5	LHN	F	44	rPPC, rTha	13
6	LHN	M	37	rPPC	10
7	LHN	F	54	rPPC, rFPC	21
8	LHN	F	53	rPPC, rTha	14
9	LHN	M	53	rPPC, rFPC, rTha, rTS	17
10	LHN	F	70	rPPC	12
11	LHN	M	56	rPPC, rFPC	10
12	LHN	F	75	rPPC, rFPC, rTha	12
13	LHN	F	57	rPPC, rTS	14
14	LHN	M	48	rPPC, rFPC	12
15	BDC	M	53	lTS, VmPFC, ACC	20
16	BDC	F	50	PFC	18
17	BDC	F	45	PFC	16
18	BDC	M	63	lTS, PFC, ACC	12
19	BDC	M	40	PFC	15
20	BDC	F	70	lPPC, lFPC	12
21	BDC	F	65	lPPC, lFPC, lTha	10
22	BDC	M	50	lPPC, FPC, lTha	12
23	BDC	F	50	FPC	12

M = male, F = female. LHN = Left Hemispatial Neglect, BDC = Brain Damaged Controls. R = right, l = left, PPC = Posterior Parietal Cortex, Tha = Thalamic nuclei, FPC = Fronto-Parietal Cortex, TS = Temporal Sulcus, PFC = PreFrontal Cortex, ACC = Anterior Cingulate Cortex; NIHSS = National Institute of Health Stroke Scale (Italian version).

Table 2
Planned comparisons in the exanimated features and variables (Aim 1).

	Variable	Statistics				Planned Comparisons
		df	t-stat	p-value	d	
Pre-stimulus Activity	*Mean IAF*	21	>3.502	<.016	>0.731*	LHN<HC;LHN<BDC
	Alpha asymmetry	13	2.303	.038	0.616	P3>P4 in LHN
	r Fronto-parietal PLI	21	>2.436	<.037	>0.518*	LHN<HC;LHN<BDC
	Inter-hemispheric PLI	26	>2.475	<.03	>0.468*	HC>LHN;HC>BDC
Post-Stimulus Processing	*vABI*	21	>3.142	<.007	>0.655*	LHN>HC;LHN>BDC
	r-l IHTT	21	>2.605	<.031	>0.555*	LHN>HC;LHN>BDC
Behavioral Asymmetry	*Bells Test*	21	>1.815	<.043	> 0.387*	LHN>BDC>HC

t-test statistics (t-stat) with degree of freedom (df), p values and Cohen's d are reported. IAF = Individual Alpha Frequency, ROIs = Regions of interest, r = right, l = left, PLI = Phase Lag Index, vABI = Visuospatial Attention Bias Index, IHTT = Inter-Hemispheric Transmission Time. LHN = Left Hemispatial Neglect, HC = Healthy Controls, BDC = Brain Damaged Controls. *Analyses are referred to multiple between-groups comparisons.

dardized scores (named Equivalent Scores, ES, range between 0 = pathological performance and 4 = performance higher than the median). The neuropsychological test battery did not reveal any pathological performance in the BDC group: Attentional matrix (M = 3; SE = 0.3) and Visual-spatial short term memory (M = 2.5; SE = 0.6) p. 13.

All participants repeated the EEG recording during four consecutive days. However, no effects of the variable repetition emerged in the alpha parameters ($F(1,147)=651$, $p=.421$, $\eta p^2=.004$), connectivity ($F(1,147)=.011$, $p=.916$, $\eta p^2=.001$) and post-stimulus measures ($F(1,147)<.948$, $p>.332$, $\eta p^2<.006$). This allowed us to exclude the effect of the repetitions over the EEG variables and to directly compare participants across repetitions.

3.1.1. Pre-stimulus features

PSD figure (Fig. 2A) showed slower IAF in the LHN group compared to the other groups. Moreover, as expected, the figure shows maximal alpha asymmetry in the LHN group, no asymmetry in the HC group, and an intermediate picture for the BDC group. This trend of groups differences is observable also in the correlation matrices of the Phase Lag Index (Fig. 2B), with minimal, intermediate, and maximal connectivity within the ROIs for LHN, BDC and HC groups respectively.

The statistical analysis of EEG on the pre-stimulus IAF confirmed a significant difference between groups with a large effect size ($F(2,34)=13.01$, $p<.001$, $\eta p^2=.449$, Fig. 2C). The planned comparisons (Table 2) specifically showed that IAF was significantly slower in the LHN group compared to HC and BDC in all considered ROIs, while no differences emerged between BDC and HC (Fig. 2C). No effect of the variable ROI emerged ($F(2,34)= 633$, $p =.514$, $\eta p^2=.019$). No significant effects of the covariates (*all ps* > .079) were found.

Similarly, analyses on between groups differences in the pre-stimulus alpha-amplitude (Fig. 2C) did not show significant effects (*all ps* > .245). Most importantly however, an asymmetry in the alpha-amplitude between right and left posterior electrodes emerged in the LHN group. Specifically, alpha-amplitude in LHN was larger over the left posterior electrode (P3) compared to the right posterior electrode (P4), while no differences were found between electrodes in the HC group and in the BDC group (all *ts*<1.737, *p*>.106, *d*<0.464, Table 2). No significant effects of the covariates (*all ps* > .511) were found.

Finally, functional connectivity was analyzed in the pre-stimulus time period. The between-subjects ANCOVA on connectivity ROIs (Fig. 2C) showed a main effect of ROI ($F(1,34)=144$, $p<.001$, $\eta p^2=.81$) and a significant interaction ROI*Group ($F(2,34)=4.76$, $p<.001$, $\eta p^2=.219$). In particular, impaired right fronto-parietal connectivity (PLI between electrodes F4-P4) emerged in the LHN group compared to the HC group and the BDC group. No differences were found between HC and BDC. Analyses additionally showed larger inter-hemispheric connectivity (PLI between electrodes P3-P4) in the HC group compared to the LHN group and the BDC group. However, no differences were found between LHN and BDC ($t(21)=0.411$, $p=.685$, $d=0.087$). Finally, no differences were found in the frontal inter-hemispheric connectivity (PLI between electrodes F3-F4) *all ps*>.382

Taken together, pre-stimulus results showed slower IAF, imbalance in the posterior alpha-amplitude and dysfunctional connectivity within the right fronto-parietal network specifically in the LHN group compared to the other control groups. Moreover, both groups of lesioned patients (LHN and BDC) showed impaired connectivity between hemispheres.

3.1.2. Post-stimulus features

Two indices derived from VEPs were investigated in the post-stimulus time period. In particular, the vABI and the IHTT reflect asymmetries in the amplitude and latency respectively in the VEPs. VEPs analyses (Fig. 3A) show the typical negative deflection after stimulus presentation with peaks around 150ms (i.e., the N100). N100, in particular, was slightly larger for left compared to right presented stimuli in the BDC and HC groups, while LHN patients show an opposite pattern. Larger amplitudes were also shown for right compared to left presented stimuli in the P300 time window, with stronger asymmetries in the LHN group. The between-subjects one-way ANCOVAs on the N100 confirmed the impression and showed an effect of group ($F(2,36)=8.722$, $p<.001$, $\eta p^2=.326$), with larger vABI in the LHN groups compared to HC and BDC, reflecting an asymmetry in perceptual processing in favor of stimuli presented in the right hemifield in the LHN patients. BDC and HC showed smaller and comparable vABI ($t(21)=0.809$, $p=.428$, $d=0.169$) (Fig. 3B). The between-subject ANCOVA on the N100 IHTT with the within subject factor direction (right to left and left to right) showed a significant Direction*Group interaction ($F(2,34)=4.893$, $p=.014$, $\eta p^2=.224$) with slower right to left transmission times in the LHN group compared to HC and BDC. No differences were found between HC and BDC ($t(21)=1.389$, $p=.179$, $d=0.392$). Analyses on left to right IHTT did not show any significant difference between groups, (*all ts*<1.567, *all ps*>.129, *all ds*<0.296, Table 2). Thus, only right to left IHTT was slower in the LHN group compared to the other control groups.

The ANCOVA on the P300 vABI shows a marginally significant effect of group ($F(2,36)=3.02$, $p=.062$, $\eta p^2=.16$) with larger bias towards right presented stimuli for LHN (P300 vABI = 2.03 μv, SE = .678 μv) compared to HC (M = 0.257 μv, SE = .422 μv) ($t(26) = 2.22$, $p=.035$, $d=0.419$). No differences emerged between LHN and BDC (1.51, SE = .619) ($t(21) = .537$, $p=.597$, $d=0.112$) and between HC and BDC ($t(21) = 1.73$, $p=.1$, $d=0.361$). Finally, the ANCOVA on the P300 IHTT did not show any significant effect (*all ps*> .437). No significant effects of the covariates in the N100 and P300 vABI and in the IHTT were found (*all ps* > .299).

3.1.3. Behavioral performance test

The between-subjects one-way ANOVA on the asymmetry score showed a significant effect of group ($F(2,34)=7.279$, $p=.002$, $\eta p^2=.287$). As expected, LHN patients committed more errors in the left hemifield (asymmetry score mean M=3.91, SE=1.01) compared to HC (M=0.446, SE=0.951) and BDC group (M=1.944, SE=0.407). Moreover,

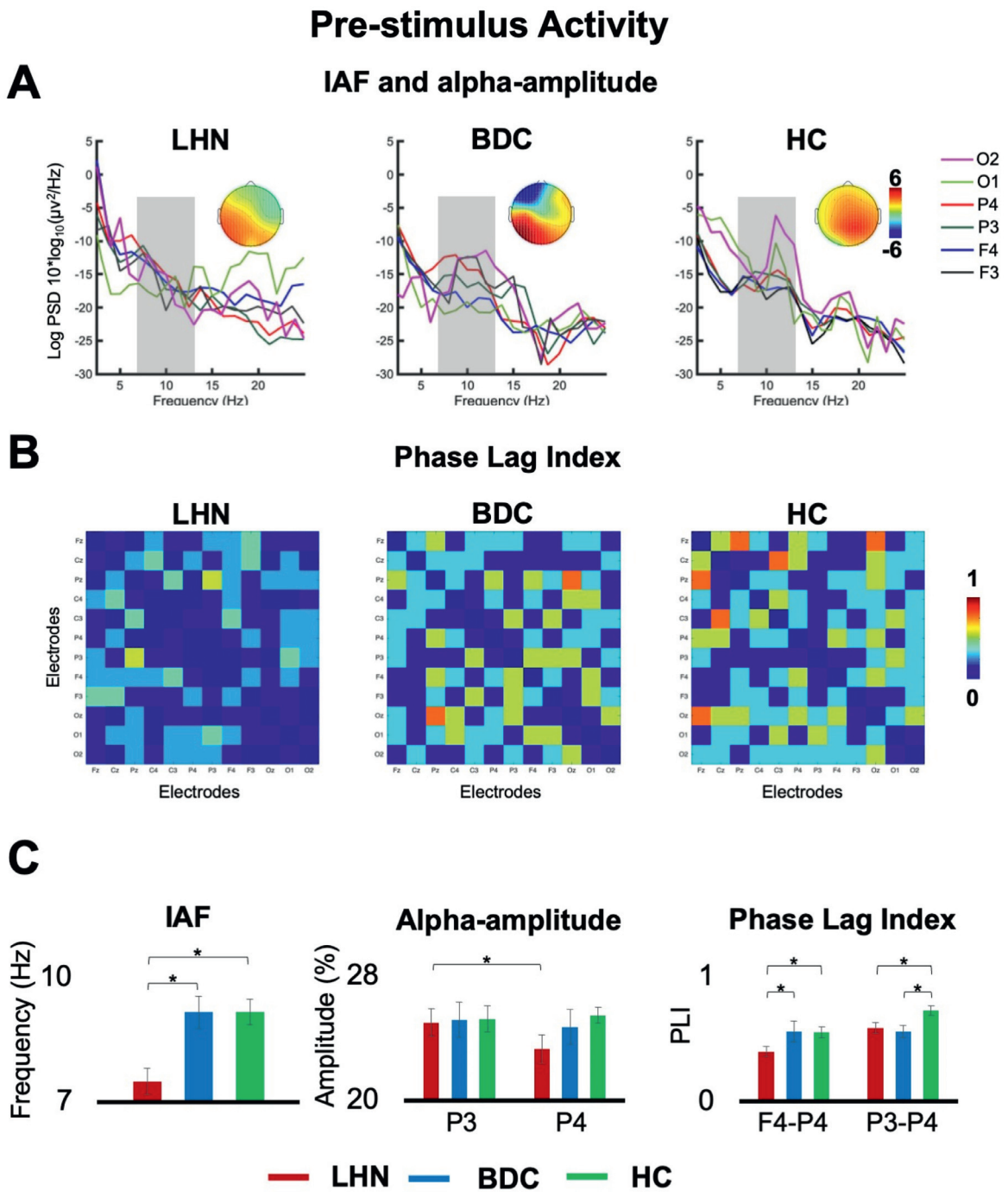

Fig. 2. Pre-stimulus activity (aim 1). A. Grand average Power spectral Density (PSD) over ROI (Regions of Interest) for the electrodes O1, O2, P3, P4, F3 and F4. Topographies show scalp distribution of alpha amplitude for the Left Hemispatial Neglect Patients (LHN), Brain Damaged Controls (BDC) and Healthy Controls (HC). Shaded areas correspond to the windows used for statistical analyses. The comparative visual assessment of spectrograms shows, respectively, maximal, intermediate and minimal asymmetry in the LHN, BDC and HC groups for the pre-stimulus IAF and alpha amplitudes. **B**. Correlation matrices of the Phase Lag Index for the three groups and over all electrodes. The visual analysis shows minimal, intermediate, and maximal connectivity within the ROIs between LHN, BDC and HC groups, respectively. **C.** Mean Individual Alpha Frequency (IAF) across ROIs for all groups, Alpha-amplitude results expressed in percentage for electrodes P3 and P4 and Phase Lag Index (PLI) results for Right fronto-parietal connectivity between electrodes F4-P4 and Inter-hemispheric connectivity between electrodes P3-P4. Two-tailed t-test statistical significance is reported ($^*p < 0.05$). Error bars represent standard error of the mean, μv = microvolt, Hz = Hertz.

BDC committed more errors compared to HC. In general, these results showed a graded modulation of the clinical performance between groups. In particular, LHN patients committed significantly more errors in the left hemifield compared to BDC and HC while BDC committed more errors only compared to HC (Table 2). No effect of test repetition emerged ($F(7,150)=0.572$, $p=.777$, $\eta p^2 = .026$).

3.2. Aim 2: To devise a causative neurophysiological model between EEG measures

For the second aim, we investigated the relationship between the most between groups discriminative EEG measures using hierarchical causative modeling. Preliminary analyses on the variables, inferred from

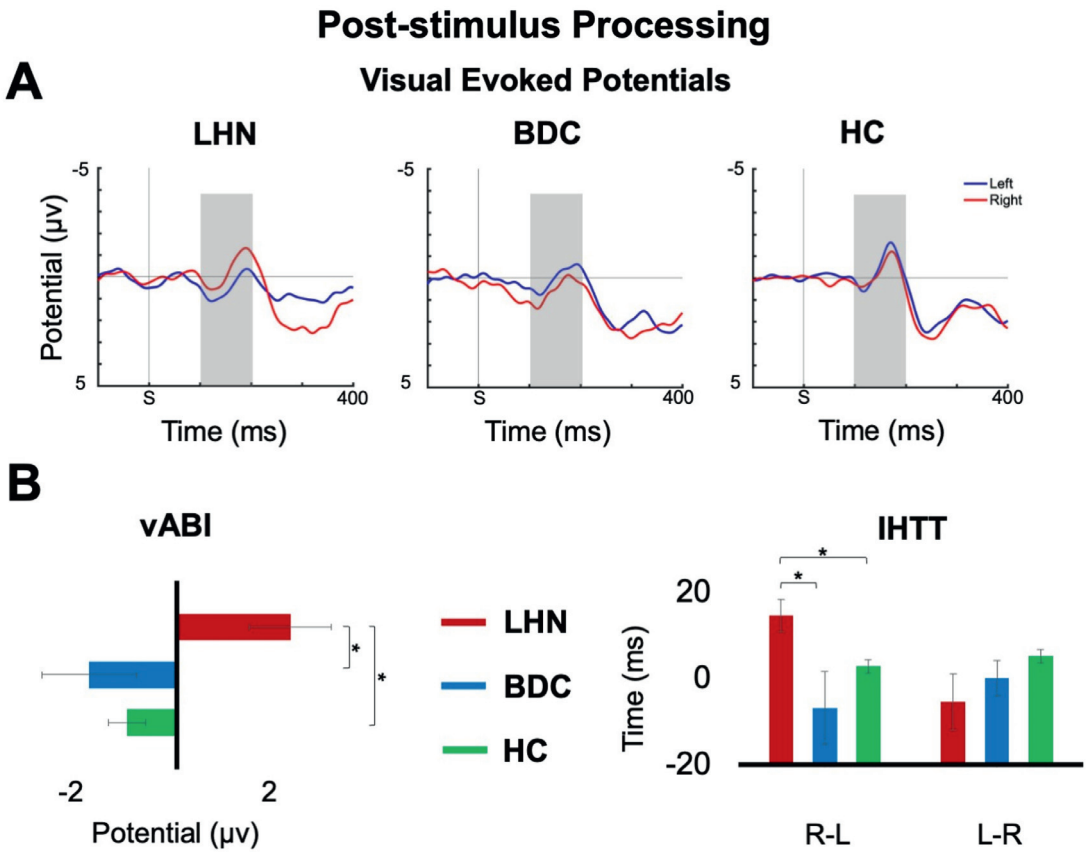

Fig. 3. Post-stimulus Processing. A. Stimulus-locked Visual evoked potentials. Grand average waveforms for left and right stimuli at the averaged electrodes P3 and P4 in healthy controls (HC), Left Hemispatial Neglect patients (LHN) and Brain Damaged Controls (BDC). **B**. N100 Visuospatial Attention Bias Index (vABI) and Inter-Hemispheric Transmission time (IHTT) results for Right to Left (R-L) and Left to Right conditions (L-R). Two-tailed t-test statistical significance is reported (*p < 0.05). Error bars represent standard error of the mean. S = time point of stimulus onset; μV = microvolt; ms = milliseconds; shaded areas correspond to the time windows used for statistical analyses.

Table 3
Shapiro-Wilk Test of Normality. The Shapiro-Wilks test detects for each EEG measure entered in the SEM analysis a difference from the normal distribution. The test rejects the hypothesis of normality when the significance level is less than or equal to .05.

	Shapiro-Wilks test Statistics	*Significance*
IAF	>.849	>.509
Alpha-amplitude	>.879	>.154
Inter-Hemispheric Connectivity	>.924	>.254
Right Fronto-Parietal Connectivity	>.950	>.559
N100 vABI	>.849	>.072
N100 IHTT	>.876	>.052

aim 1 results, showed that all EEG measures were normally distributed (see Table 3).

Thus, three pre-stimulus variables were considered for the refined model: (1) *Perceptual sampling*, which is expressed by a single indicator (i.e., mean IAF across all ROIs); (2) *Attention distribution*, which is expressed by the alpha-amplitude over the right parietal electrode; and, (3) *Connectivity within the visuospatial perceptual network*, which is expressed by PLI over P3-P4 and over F4-P4. In the post-stimulus time, we considered: (1) *stimulus processing bias* (expressed by the N100 vABI and P300 vABI) and (2) *latency* (expressed by the right to left N100 IHTT). Finally, *behavioral asymmetry* was expressed by the asymmetry score in the Bells test. Indicators from 151 EEG (3 EEG with strong artifacts were excluded) were extracted and entered the model (Fig. 4A).

The Fig. 4 shows the initial hypothesized model, the refined model with the results of aim 1 and the final model based on SEM analyses. Model fit statistics showed acceptable overall model assessment (χ^2 not significant; RMSEA=.001; SRMR=.037 Fig. 4). Internal consistency reliability (mean Cronbach Alpha=.926) was acceptable for single subject measurements (>.850). Moreover, indicators represented only one underlying latent variable (AVE>.686). Bootstrap loadings showed supra-threshold (0.40) discriminant validity for the variable connectivity, which has more then one indicator (PLI P3-P4 loading=.896, PLI F4-P4 loading=.707). However, loadings showed under-threshold discriminant validity for the indicator P300 vABI (loading=.289) and supra-threshold validity for the indicator N100 vABI (loading=.931). Thus, the P300 vABI was excluded in the final model.

Results of the associations among variables are reported in Table 4 with path coefficients (sample and bootstrap estimations), t-values and 95% confidence intervals. Results showed a significant pathway linking pre-stimulus IAF and connectivity with post-stimulus vABI, predicting the asymmetry score. While this pathway reflects the impact of pre-stimulus IAF and connectivity over post-stimulus vABI to predict behavioral performance, results additionally showed a direct link between pre-stimulus alpha-amplitude and behavioral performance. Together, these two pathways explain 83.08% of the variance in the asymmetry score of the Bells test (Fig. 4B). Analyses finally show an association between connectivity and IHTT, but no significant links were found with the behavioral performance.

The model was further validated considering the scores from other behavioral measures for the assessment of LHN cognitive (i.e., the Fluff Test and the Picture Scanning) and motor functioning (i.e., the MI). SRMR results showed good model fit for both cognitive (all SRMR < .0431), and motor functioning tests (SRMR = .0419).

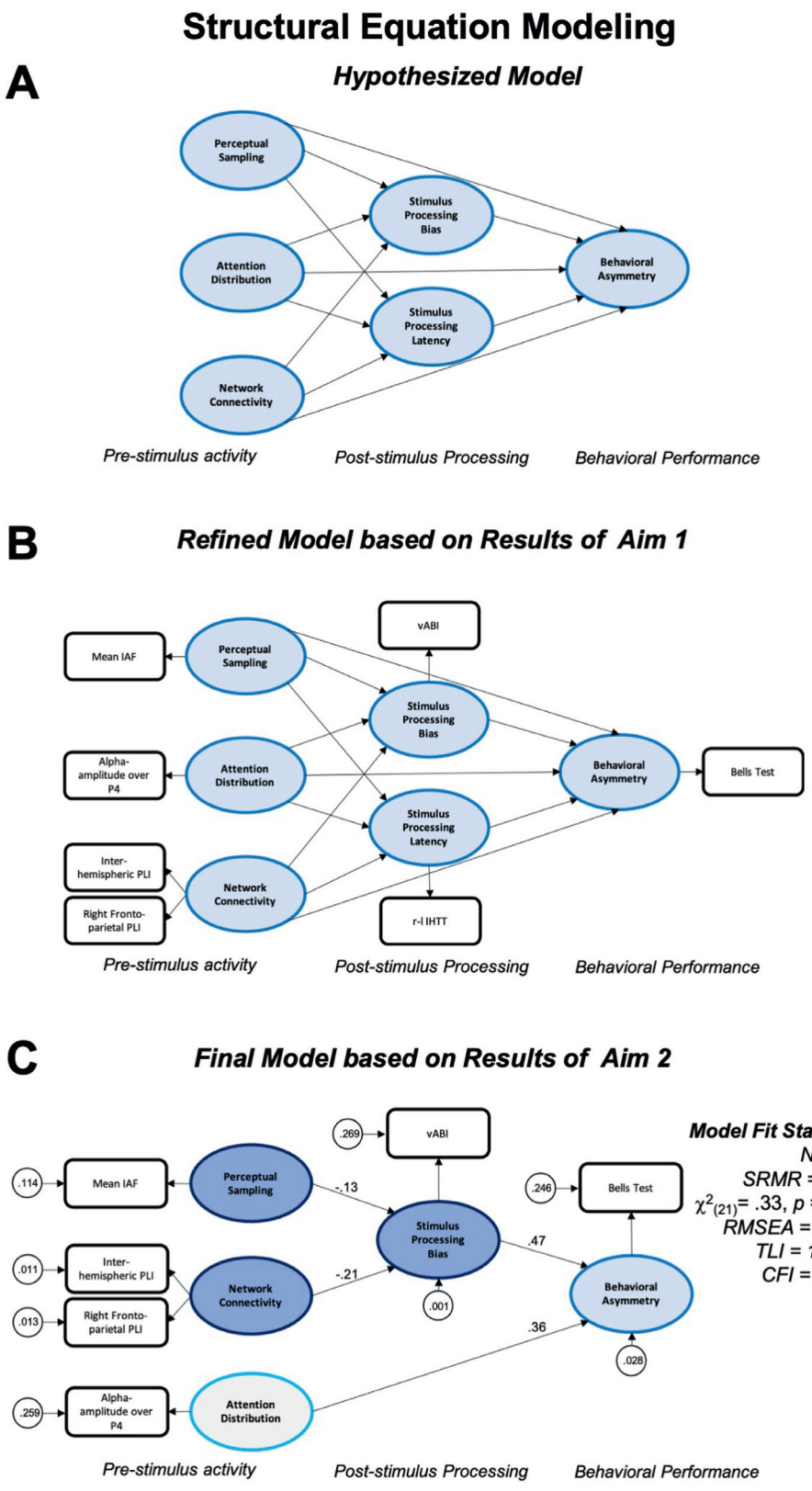

Fig. 4. Structural Equation Modeling (SEM). A. Original Hypothesized causative associations between latent variables (ellipses). **B.** Refined model and indicators definition (rectangles) based on results of between-subjects analyses (aim 1). **C.** Final model optimization based on SEM results (aim 2). Arrows reflect associations (i.e., pathways) between latent variables and between variables and indicators. The relative variance explained by each pathway is reported on the regression arrow and errors of measurement are represented as circles for both indicator and second-order latent variables. Results of model fit statistics are reported and * represent acceptable and good fit**. IAF = Individual Alpha Frequency, PLI = Phase Lag Index, r-l IHTT = right to left Inter-Hemispheric Transmission Time, vABI = Visuo-spatial Attention Bias Index, N = sample size, χ^2 = chi squared with degree of freedom in brackets and p value, SRMR = Standardized Root Mean square Residual, RMSEA = Root Mean Square Error of Approximation, TLI = Tucker-Lewis Index, CFI = Comparative Fit Index.

4. Discussion

Many studies have focused on EEG indices of visuospatial perception and some of these indices are considered potential biomarkers of LHN (Deouell et al., 2000; Di Russo et al., 2013, 2008; Doricchi et al., 2008; He et al., 2007; Lasaponara et al., 2019, 2018; Verleger et al., 1996). The main purpose of the present study was to investigate the causal association between these EEG biomarkers to understand how these relationships could predict clinical outcomes of LHN. To this aim, we recorded EEG during lateralized stimuli presentation, where no mo-

Table 4
Paths coefficients results (Aim 2).

		Sample Estimation	Bootstrap Estimation	t-stat	p-value	CI LB	CI UB
Pre-stimulus Activity	*IAF → vABI*	-.135	-.127	-1.686	.047	-.302	-.005
	IAF → IHTT	.138	.132	1.544	n.s.	-.01	.344
	IAF → Bells Test	-.041	-.038	-0.461	n.s.	-.23	.125
	Alpha-amplitude→vABI	-.111	-.106	-1.515	n.s.	-.262	.028
	Alpha-amplitude→IHTT	.061	.059	0.732	n.s.	-.119	.222
	Alpha-amplitude→BellsTest	.34	.346	3.513	<.001	.149	.506
	Connectivity → vABI	-.234	-.231	-4.466	<.001	-.342	-.139
	Connectivity → IHTT	.288	.285	3.796	<.001	.161	.469
	Connectivity → Bells Test	-.204	-.213	-3.087	<.001	-.323	-.054
Post-Stimulus Processing	*vABI → Bells Test*	.461	.462	6.938	<.001	.333	.597
	IHTT → Bells Test	.036	.042	0.584	n.s.	-.092	.148

Path Coefficients are reported for all considered associations in the model as sample and bootstrap estimations, t-stats, relative p-values and lower (LB) and uper (UB) bounds of the 95% confidence intervals. IAF = Individual Alpha Frequency, IHTT = Inter-Hemispheric Transmission Time, vABI = Visuospatial Attention Bias Index, n.s. = not significant.

tor responses were required, in LHN patients and controls. This allowed us to directly investigate asymmetries in the visuospatial abilities and in the processing of lateralized stimuli between groups. Then, we used the SEM to generate a neurophysiological hierarchical causative model between the EEG correlates of visuospatial perception. The SEM model was able to identify psychophysiological pathways behind visuospatial perception and to describe how these pathways can predict perceptual performance in LHN and controls. In particular, the model identified an indirect and a direct pathway, highlighting a possible structure of visuospatial perception abilities. Notably, these two pathways can collectively explain more than 80% of the variance in the perceptual asymmetry index.

The indirect pathway of the model is a two-stages pathway, linking pre-stimulus anticipatory IAF and connectivity within the fronto-parietal perceptual network with post-stimulus processing bias (as expressed by the vABI). Here, impaired connectivity and slower IAF as observed in LHN are related to a right bias in stimulus processing. Importantly, these associations predict more perceptual misses over the left hemifield in the Bells test. As previously hypothesized, anticipatory IAF seems to play a crucial role in visuospatial perception (Babiloni et al., 2006; Di Gregorio et al., 2022a; Samaha and Postle, 2015; Thut et al., 2006; Trajkovic et al., 2021; Zazio et al., 2020). Specifically, trial by trial variability of IAF can account for the individual ability to accurately perceive incoming stimuli and sample sensory information. In this sense, IAF may be conceived as the time unit or temporal window within which sensory information can be integrated (Bertaccini et al., 2022; Di Gregorio et al., 2022c; Trajkovic et al., 2022). Thus, faster IAF may reflect a more efficient perceptual sampling and a fine grained sensorial processing (Di Gregorio et al., 2022c; Iemi et al., 2019; Samaha and Postle, 2015; Wutz et al., 2018). Accordingly, slower IAF might impair perceptual resolution by creating less sampling frames per sensory processing. Moreover, as reported in previous studies, connectivity is enhanced in the healthy population during spatial attentional task within the fronto-parietal network (Hembrook Short et al., 2017; Hembrook-Short et al., 2019) and this connectivity predicts perceptual sensitivity and metacognitive abilities (Chiappini et al., 2022, 2018; Di Luzio et al., 2022; Romei et al., 2016). Our results confirm this view; indeed, better inter-hemispheric and right intra-hemispheric communications can facilitate information flow within a visuospatial perception network, thus empowering lateralized stimulus processing (Chiappini et al., 2022). On the other hand, lower right intra-hemispheric connectivity in LHN patients is related to impaired processing of contralesional stimuli. Importantly, however, Neglect can also occur after left hemispheric lesions (rates between 18-30%) (Esposito et al., 2021). Although, we did not enroll patients with left stroke etiology, we can hypostasize that intra and inter-hemispheric connectivity and perceptual processing could differ between these sub-groups of Neglect patients.

The IAF and connectivity create together a functional link with post-stimulus processing bias (as indexed by the vABI). In particular, the vABI reflects the difference in the activation of the inter-hemispheric network between stimuli presented in the right and in the left hemifields. In HC and BDC, the vABI is around 0, thus demonstrating similar responses to left and right presented stimuli. Differently, in the LHN group, a positive vABI indicates an imbalance in perceptual resources allocation and a bias in the stimulus processing towards the right hemifield. The perceptual processing in LHN is not only biased but also delayed. Indeed, IHTT results showed that information sharing, within the inter-hemispheric network in LHN, was slower (see also Di Gregorio et al. (2022b, 2020)). However, BDC showed a similar delay and impaired connectivity within the inter-hemispheric network. These last results are presumably related to the effects induced by the lesions over the inter-hemispheric communication. It is important to notice that brain damage sites differed between BDC and LHN, as lesions were allocated over the left and the right hemispheres respectively. Thus, it is possible to hypothesize that dysfunctional inter-hemispheric communications in the BDC and LHN patients are caused by different lesion locations.

In general, the indirect pathway of the model links anticipatory activity to behavioral asymmetries via post-stimulus activity. Specifically, pre-stimulus IAF may reflect perceptual sampling (Busch and VanRullen, 2010; VanRullen, 2016) and the connectivity level could reflect the ability of the perceptual system to share information (Dehaene et al., 2014; King et al., 2013). These two measures are closely related and together predict the post-stimulus vABI. Hence, in this context, the vABI may reflect, in one single index, the distribution of perceptual resources within the system. Accordingly, in LHN patients, where sensory sampling and right hemisphere connectivity are impaired, a positive vABI indicates impaired stimulus-processing for left incoming stimuli. This ultimately leads to biased behavioral performance.

The model additionally showed a second direct pathway, linking the alpha-amplitude distribution and the behavioral asymmetries. Previous studies suggested that, the hemispheric distribution of pre-stimulus alpha-amplitude accounts for attentive resources allocation (Capotosto et al., 2009; Peylo et al., 2021; Thut et al., 2006). Specifically, larger alpha-amplitude in one hemisphere reflects a contralateral locus of attention (Capotosto et al., 2009; Corbetta and Shulman, 2002; Lasaponara et al., 2019; Romei et al., 2008; Thut et al., 2006). In this sense, alpha-amplitude and the direct pathway may reflect the laterality of attentive resources allocation, influencing behavioral performance. This result is in line with theories conceiving hemispheric imbalance as the neural substrate of the cognitive and behavioral symptoms of LHN (Baldassarre et al., 2014; Bartolomeo, 2021; Bartolomeo et al., 2007; Làdavas et al., 1997). Specifically, in LHN an injury of the right parietal area does not only depress the activity of this area, but also causes disinhibition of the homolog areas of the left hemisphere (Corbetta and

Shulman, 2011; Kinsbourne, 1987). Within this theoretical framework, overactivation of the left hemisphere may bias the locus of attention towards the right hemifield (Doesburg et al., 2009; Klimesch et al., 2007; Romei et al., 2008), via an inhibitory effect of the left hemisphere over the lesioned one (Baldassarre et al., 2016, 2014; Carter et al., 2010; Corbetta et al., 2005; Làdavas et al., 1997; Lasaponara et al., 2019).

The empirical associations found in the model have important clinical and experimental implications. Indeed, the model indicators have demonstrated high reliability in discriminating patients with behavioral asymmetries, and can be used for the assessment of LHN in clinical contexts. Moreover, the model can be considered as a theoretical, empirically tested, framework to formulate hypotheses about psychophysiological functioning in LHN and perceptual disorders. In general, a putative interpretation of the model results and of the cognitive functions underlying the pathways may suggest that alpha-amplitude reflects attentive resources distribution, while IAF, connectivity and vABI together may reflect stimulus-processing capacities. Thus, we could hypothesize that the pathways presumably reflect two distinct pathological clusters in LHN which are respectively related to attentive (Capotosto et al., 2009; Lasaponara et al., 2019) and stimulus processing impairments (Deouell et al., 2000; Di Russo et al., 2008).

The study results should be considered in the light of some limitations. Our results showed that the the model can be generalized to other behavioral measures assessing cognitive (i.e., Fluff Test and Picture Scanning test) and motor symptoms (i.e., MI in the right limbs) of LHN. However, a larger assessment may help to identify possible functional dissociations between the two model pathways. Moreover, we analyzed EEG repetitions across subjects and demonstrated the absence of repetition dependency effect in the ANCOVA. However, the ANCOVA and the SEM are two statistically different models and repetion dependency in the SEM still needs further testing. For instance, a larger sample size within a multicentrinc study with single subject data could be used to confirm the model without repeated measurements. Finally, external validations of the model would be necessary to test the model applicability in LHN rehabilitation. For instance, a direct manipulation of the model pathways, by the use of specific rehabilitation protcols, may test the model sensitivity to post-treatment induced changes. Our study is a preliminary application of the SEM model for the study of Neglect and visuospatial perception and can represent a reference for future validations of the model and sample size calculations.

5. Conclusions

The present study and the proposed model can offer an empirical framework to drive hypothesis on the psychophysiological functioning of perceptual disorders. Moreover, the model allows to test assumptions about psychophysiological effects of innovative or existing protocols for the rehabilitation of perceptual disorders.

Funding

F.D.G. is supported by the Ministero della Salute (SG-2018-12367527) and V.R. is supported by the Bial Foundation (204/18). The publication of this article was supported by the "Ricerca Corrente" funding from the Italian Ministry of Health.

Declaration of Competing Interest

Authors declare no competing interests.

Credit authorship contribution statement

Francesco Di Gregorio: Conceptualization, Methodology, Formal analysis, Writing – original draft, Visualization. **Valeria Petrone:** Conceptualization, Methodology, Investigation, Writing – review & editing. **Emanuela Casanova:** Methodology, Investigation, Project administration, Writing – review & editing. **Giada Lullini:** Supervision, Writing – review & editing. **Vincenzo Romei:** Supervision, Writing – review & editing. **Roberto Piperno:** Supervision, Writing – review & editing. **Fabio La Porta:** Conceptualization, Methodology, Project administration, Supervision, Writing – review & editing.

Data availability

Data will be made available on request.

Acknowledgements

The authors are grateful to all the Neurorehabilitation Unit staff of the Maggiore Hospital and Villa Bellombra Hospital for logistic and work support.

References

Aria, M., Capaldo, G., Iorio, C., Orefice, C.I., Riccardi, M., Siciliano, R., 2018. PLS path modeling for causal detection of project management skills: a research field in national research council in Italy. Electron. J. Appl. Stat. Anal. 11, 516–545. doi:10.1285/i20705948v11n2p516.

Babiloni, C., Barry, R.J., Başar, E., Blinowska, K.J., Cichocki, A., Drinkenburg, W.H.I.M., Klimesch, W., Knight, R.T., Lopes da Silva, F., Nunez, P., Oostenveld, R., Jeong, J., Pascual-Marqui, R., Valdes-Sosa, P., Hallett, M., 2020. International Federation of Clinical Neurophysiology (IFCN) – EEG research workgroup: Recommendations on frequency and topographic analysis of resting state EEG rhythms. Part 1: applications in clinical research studies. Clin. Neurophysiol. 131, 285–307. doi:10.1016/j.clinph.2019.06.234.

Babiloni, C., Vecchio, F., Bultrini, A., Romani, G.L., Rossini, P.M., 2006. Pre- and poststimulus alpha rhythms are related to conscious visual perception: a high-resolution EEG study. Cereb. Cortex 16, 1690–1700. doi:10.1093/cercor/bhj104.

Baldassarre, A., Ramsey, L., Hacker, C.L., Callejas, A., Astafiev, S.V., Metcalf, N.V., Zinn, K., Rengachary, J., Snyder, A.Z., Carter, A.R., Shulman, G.L., Corbetta, M., 2014. Large-scale changes in network interactions as a physiological signature of spatial neglect. Brain 137, 3267–3283. doi:10.1093/brain/awu297.

Baldassarre, A., Ramsey, L., Rengachary, J., Zinn, K., Siegel, J.S., Metcalf, N.V., Strube, M.J., Snyder, A.Z., Corbetta, M., Shulman, G.L., 2016. Dissociated functional connectivity profiles for motor and attention deficits in acute right-hemisphere stroke. Brain 139, 2024–2038. doi:10.1093/brain/aww107.

Bartolomeo, P., 2021. From competition to cooperation: Visual neglect across the hemispheres. Rev. Neurol. 177, 1104–1111. doi:10.1016/j.neurol.2021.07.015, (Paris), THEMATIC SECTION: PLASTICITY.

Bartolomeo, P., Thiebaut De Schotten, M., Chica, A.B., 2012. Brain networks of visuospatial attention and their disruption in visual neglect. Front. Hum. Neurosci. 6, 110. doi:10.3389/fnhum.2012.00110.

Bartolomeo, P., Thiebaut de Schotten, M., Doricchi, F., 2007. Left unilateral neglect as a disconnection syndrome. Cereb. Cortex 17, 2479–2490. doi:10.1093/cercor/bhl181.

Bell, A., Sejnowski, T., 1995. An information-maximization approach to blind separation and blind deconvolution. Neural Comput. 7, 1129–1159. doi:10.1162/neco.1995.7.6.1129.

Bentler, P.M., Yuan, K.H., 1999. Structural equation modeling with small samples: test statistics. Multivar. Behav. Res. 34, 181–197. doi:10.1207/S15327906Mb340203.

Bertaccini, R., Ellena, G., Macedo-Pascual, J., Carusi, F., Trajkovic, J., Poch, C., Romei, V., 2022. Parietal alpha oscillatory peak frequency mediates the effect of practice on visuospatial working memory performance. Vision. 6, 30. doi:10.3390/vision6020030.

Briggs, F., Mangun, G.R., Usrey, W.M., 2013. Attention enhances synaptic efficacy and the signal-to-noise ratio in neural circuits. Nature 499, 476–480. doi:10.1038/nature12276.

Brighina, F., Bisiach, E., Oliveri, M., Piazza, A., Bua, V.L., Daniele, O., Fierro, B., 2003. 1 Hz repetitive transcranial magnetic stimulation of the unaffected hemisphere ameliorates contralesional visuospatial neglect in humans. Neurosci. Lett. 336, 131–133. doi:10.1016/S03.

Brown, W.S., Larson, E.B., Jeeves, M.A., 1994. Directional asymmetries in interhemispheric transmission time: evidence from visual evoked potentials. Neuropsychologia 32, 439–448. doi:10.1016/0028-3932(94)90089-2.

Busch, N.A., VanRullen, R., 2010. Spontaneous EEG oscillations reveal periodic sampling of visual attention. Proc. Natl. Acad. Sci. 107, 16048–16053. doi:10.1073/pnas.1004801107.

Byrne, B.M., 2011. Structural Equation Modeling with Mplus Basic Concepts, Applications. Routledge, New York ed..

Campos Viola, F., Thorne, J., Edmonds, B., Schneider, T., Eichele, T., Debener, S., 2009. Semi-automatic identification of independent components representing EEG artifact. Clin. Neurophysiol. 120, 868–877. doi:10.1016/j.clinph.2009.01.015.

Cangur, S., Ercan, I., 2015. Comparison of model fit indices used in structural equation modeling under multivariate normality. J. Mod. Appl. Stat. Methods 14, 152–167. doi:10.22237/jmasm/1430453580.

Capotosto, P., Babiloni, C., Romani, G.L., Corbetta, M., 2009. Frontoparietal cortex controls spatial attention through modulation of anticipatory alpha rhythms. J. Neurosci. 29, 5863–5872. doi:10.1523/JNEUROSCI.0539-09.2009.

Carter, A.R., Astafiev, S.V., Lang, C.E., Connor, L.T., Rengachary, J., Strube, M.J., Pope, D.L.W., Shulman, G.L., Corbetta, M., 2010. Resting interhemispheric functional magnetic resonance imaging connectivity predicts performance after stroke. Ann. Neurol. 67, 365–375. doi:10.1002/ana.21905.

Cecere, R., Rees, G., Romei, V., 2015. Individual differences in alpha frequency drive cross-modal illusory perception. Curr. Biol. 25, 231–235. doi:10.1016/j.cub.2014.11.034.

Chiappini, E., Sel, A., Hibbard, P.B., Avenanti, A., Romei, V., 2022. Increasing interhemispheric connectivity between human visual motion areas uncovers asymmetric sensitivity to horizontal motion. Curr. Biol. doi:10.1016/j.cub.2022.07.050.

Chiappini, E., Silvanto, J., Hibbard, P.B., Avenanti, A., Romei, V., 2018. Strengthening functionally specific neural pathways with transcranial brain stimulation. Curr. Biol. 28, R735–R736. doi:10.1016/j.cub.2018.05.083.

Coldea, A., Veniero, D., Morand, S., Trajkovic, J., Romei, V., Harvey, M., Thut, G., 2022. Effects of rhythmic transcranial magnetic stimulation in the alpha-band on visual perception depend on deviation from alpha-peak frequency: faster relative transcranial magnetic stimulation alpha-pace improves performance. Front. Neurosci. 16, 886342. doi:10.3389/fnins.2022.886342.

Cooke, J., Poch, C., Gillmeister, H., Costantini, M., Romei, X., 2019. Oscillatory properties of functional connections between sensory areas mediate cross-modal illusory perception. J. Neurosci. 39, 5711–5718.

Corbetta, M., Kincade, M.J., Lewis, C., Snyder, AZ, Sapir, A., 2005. Neural basis and recovery of spatial attention deficits in spatial neglect. Nat. Neurosci. 8, 1603–1610. doi:10.1038/nn1574.

Corbetta, M., Shulman, G.L., 2011. Spatial neglect and attention networks. Annu. Rev. Neurosci. doi:10.1146/annurev-neuro-061010-113731.

Corbetta, M., Shulman, G.L., 2002. Control of goal-directed and stimulus-driven attention in the brain. Nat. Rev. Neurosci. 3, 201–215. doi:10.1038/nrn755.

Dambeck, N., Sparing, R., Meister, I.G., Wienemann, M., Weidemann, J., Topper, R., Boroojerdi, B., 2006. Interhemispheric imbalance during visuospatial attention investigated by unilateral and bilateral TMS over human parietal cortices. Brain Res. 1072, 194–199. doi:10.1016/j.brainres.2005.05.075.

Dehaene, S., Charles, L., King, J.R., Marti, S., 2014. Toward a computational theory of conscious processing. Curr. Opin. Neurobiol. 25, 76–84. doi:10.1016/j.conb.2013.12.005.

Delorme, A., Makeig, S., 2004. EEGLAB: an open source toolbox for analysis of single-trial EEG dynamics including independent component analysis. J. Neurosci. Methods 134, 9–21. doi:10.1016/j.jneumeth.2003.10.009.

Deouell, L.Y., Hämäläinen, H., Bentin, S., 2000. Unilateral neglect after right-hemisphere damage: contributions from event-related potentials. Audiol. Neurootol. 5, 225–234. doi:10.1159/000013884.

Di Gregorio, F., La Porta, F., Casanova, E., Magni, E., Bonora, R., Ercolino, M.G., Petrone, V., Leo, M.R., Piperno, R., 2021a. Efficacy of repetitive transcranial magnetic stimulation combined with visual scanning treatment on cognitive and behavioral symptoms of left hemispatial neglect in right hemispheric stroke patients: study protocol for a randomized controlled trial. Trials 22, 1–11. doi:10.1186/s13063-020-04943-6.

Di Gregorio, F., La Porta, F., Lullini, G., Casanova, E., Petrone, V., Simoncini, L., Ferrucci, E., Piperno, R., 2021b. Efficacy of repetitive transcranial magnetic stimulation combined with visual scanning treatment on cognitive-behavioral symptoms of unilateral spatial neglect in patients with traumatic brain injury: study protocol for a randomized controlled trial. Front. Neurol. 0. doi:10.3389/fneur.2021.702649.

Di Gregorio, F., La Porta, F., Petrone, V., Battaglia, S., Orlandi, S., Ippolito, G., Romei, V., Piperno, R., Lullini, G., 2022a. Accuracy of EEG biomarkers in the detection of clinical outcome in disorders of consciousness after severe acquired brain injury: preliminary results of a pilot study using a machine learning approach. Biomedicines 10, 1897. doi:10.3390/biomedicines10081897.

Di Gregorio, F., Maier, M.E., Steinhauser, M., 2022b. Early correlates of error-related brain activity predict subjective timing of error awareness. Psychophysiology 00. doi:10.1111/psyp.14020.

Di Gregorio, F., Maier, M.E., Steinhauser, M., 2020. Are errors detected before they occur? Early error sensations revealed by metacognitive judgments on the timing of error awareness. Conscious. Cogn. 77, 102857. doi:10.1016/j.concog.2019.102857.

Di Gregorio, F., Trajkovic, J., Roperti, C., Marcantoni, E., Di Luzio, P., Avenanti, A., Thut, G., Romei, V., 2022c. Tuning alpha rhythms to shape conscious visual perception. Curr. Biol. 0. doi:10.1016/j.cub.2022.01.003.

Di Luzio, P., Tarasi, L., Silvanto, J., Avenanti, A., Romei, V., 2022. Human perceptual and metacognitive decision-making rely on distinct brain networks. PLoS Biol. 20, e3001750. doi:10.1371/journal.pbio.3001750.

Di Russo, F., Aprile, T., Spitoni, G., Spinelli, D., 2008. Impaired visual processing of contralesional stimuli in neglect patients: a visual-evoked potential study. Brain 131, 842–854. doi:10.1093/brain/awm281.

Di Russo, F., Bozzacchi, C., Matano, A., Spinelli, D., 2013. Hemispheric differences in VEPs to lateralised stimuli are a marker of recovery from neglect. Cortex 49, 931–939. doi:10.1016/j.cortex.2012.04.017.

Doesburg, S.M., Green, J.J., McDonald, J.J., Ward, L.M., 2009. From local inhibition to long-range integration: a functional dissociation of alpha-band synchronization across cortical scales in visuospatial attention. Brain Res. 1303, 97–110. doi:10.1016/j.brainres.2009.09.069.

Doricchi, F., Pinto, M., Pellegrino, M., Marson, F., Aiello, M., Campana, S., Tomaiuolo, F., Lasaponara, S., 2021. Deficits of hierarchical predictive coding in left spatial neglect. Brain Commun. 3, fcab111. doi:10.1093/braincomms/fcab111.

Doricchi, F., Thiebaut de Schotten, M., Tomaiuolo, F., Bartolomeo, P., 2008. White matter (dis)connections and gray matter (dys)functions in visual neglect: gaining insights into the brain networks of spatial awareness. Cortex 44, 983–995. doi:10.1016/j.cortex.2008.03.006.

Esposito, E., Shekhtman, G., Chen, P., 2021. Prevalence of spatial neglect post-stroke: a systematic review. Ann. Phys. Rehabil. Med. 64, 101459. doi:10.1016/j.rehab.2020.10.010.

Giaquinto, S., Cobianchi, A., Macera, F., Nolfe, G., 1994. EEG Recordings in the course of recovery from stroke. Stroke 25, 2204–2209. doi:10.1161/01.STR.25.11.2204.

Gibbons, C., Thornton, E., Ealing, J., Shaw, P., Talbot, K., Tennant, A., Young, C., 2013. The impact of fatigue and psychosocial variables on quality of life for patients with motor neuron disease. Amyotroph. Lateral Scler. Frontotemporal Degener. 14, 537–545. doi:10.3109/21678421.2013.799700.

Greenhouse, S.W., Geisser, S., 1959. On methods in the analysis of profile data. Psychometrika 24, 95–112. doi:10.1007/BF02289823.

Hair, J.F., Sarstedt, M., Hopkins, L., Kuppelwieser, V.G., 2014. Partial least squares Structural Equation Modeling (PLS-SEM): an emerging tool in business research. Eur. Bus. Rev. 26, 106–121. doi:10.1108/EBR-10-2013-0128.

Hardmeier, M., Hatz, F., Bousleiman, H., Schindler, C., Stam, C.J., Fuhr, P., 2014. Reproducibility of functional connectivity and graph measures based on the phase lag index (PLI) and weighted phase lag index (wPLI) derived from high resolution EEG. PLoS One 9. doi:10.1371/journal.pone.0108648.

He, B.J., Snyder, A.Z., Vincent, J.L., Epstein, A., Shulman, G.L., Corbetta, M., 2007. Breakdown of functional connectivity in frontoparietal networks underlies behavioral deficits in spatial neglect. Neuron 53, 905–918. doi:10.1016/j.neuron.2007.02.013.

Hembrook Short, J.R., Mock, V.L., Briggs, F., 2017. Attentional modulation of neuronal activity depends on neuronal feature selectivity. Curr. Biol. 27, 1878–1887. doi:10.1016/j.cub.2017.05.080, e5.

Hembrook-Short, J.R., Mock, V.L., Usrey, W.M., Briggs, F., 2019. Attention enhances the efficacy of communication in V1 local circuits. J. Neurosci. 39, 1066–1076. doi:10.1523/JNEUROSCI.2164-18.2018.

Husain, M., Nachev, P., 2007. Space and the parietal cortex. Trends Cogn. Sci. 11, 30–36. doi:10.1016/j.tics.2006.10.011.

Husain, M., Rorden, C., 2003. Non-spatially lateralized mechanisms in hemispatial neglect. Nat. Rev. Neurosci. 4, 26–36. doi:10.1038/nrn1005.

Iemi, L., Busch, N.A., Laudini, A., Haegens, S., Samaha, J., Villringer, A., Nikulin, V.V., 2019. Multiple mechanisms link prestimulus neural oscillations to sensory responses. eLife 8, 1–34. doi:10.7554/eLife.43620.001.

Ippolito, G., Bertaccini, R., Tarasi, L., Di Gregorio, F., Trajkovic, J., Battaglia, S., Romei, V., 2022. The role of alpha oscillations among the main neuropsychiatric disorders in the adult and developing human brain: evidence from the last 10 years of research. Biomedicines 10, 3189. doi:10.3390/biomedicines10123189.

Jacquin-Courtois, S., 2015. Hemi-spatial neglect rehabilitation using non-invasive brain stimulation: Or how to modulate the disconnection syndrome? Ann. Phys. Rehabil. Med. 58, 251–258. doi:10.1016/j.rehab.2015.07.388.

Jutten, C., Herault, J., 1991. Blind separation of sources, part I: An adaptive algorithm based on neuromimetic architecture. Signal Process. 24, 1–10. doi:10.1016/0165-1684(91)90079-X.

King, J.R., Sitt, J.D., Faugeras, F., Rohaut, B., El Karoui, I., Cohen, L., Naccache, L., Dehaene, S., 2013. Information sharing in the brain indexes consciousness in noncommunicative patients. Curr. Biol. 23, 1914–1919. doi:10.1016/j.cub.2013.07.075.

Kinsbourne, M., 1987. Mechanisms of unilateral neglect. In: Jeannerod, M. (Ed.), Advances in Psychology. North-Holland, pp. 69–86. doi:10.1016/S0166-4115(08)61709-4.

Klimesch, W., Sauseng, P., Hanslmayr, S., 2007. EEG alpha oscillations: the inhibition-timing hypothesis. Brain Res. Rev. 53, 63–88. doi:10.1016/j.brainresrev.2006.06.003.

Koch, G., Bonnì, S., Giacobbe, V., Bucchi, G., Basile, B., Lupo, F., Versace, V., Bozzali, M., Caltagirone, C., 2012. Theta-burst stimulation of the left hemisphere accelerates recovery of hemispatial neglect. Neurology 78, 24–30. doi:10.1212/WNL.0b013e31823ed08f.

Koechlin, E., Ody, C., Kouneiher, F., 2003. The architecture of cognitive control in the human prefrontal cortex. Science 302, 1181–1185.

Koshiyama, D., Thomas, M.L., Miyakoshi, M., Joshi, Y.B., Molina, J.L., Tanaka-Koshiyama, K., Sprock, J., Braff, D.L., Swerdlow, N.R., Light, G.A., 2021. Hierarchical Pathways from Sensory Processing to Cognitive, Clinical, and Functional Impairments in Schizophrenia. Schizophr. Bull. 47, 373–385. doi:10.1093/schbul/sbaa116.

Làdavas, E., Berti, A., Ruozzi, E., Barboni, F., 1997. Neglect as a deficit determined by an imbalance between multiple spatial representations. Exp. Brain Res. 116, 493–500. doi:10.1007/PL00005777.

Ladavas, E., Del Pesce, M., Provinciali, L., 1987. Unilateral attention deficits and hemispheric asymetries in the control of attention. Neuropsychologia 27, 353–366.

Lasaponara, S., D'Onofrio, M., Pinto, M., Aiello, M., Pellegrino, M., Scozia, G., De Lucia, M., Doricchi, F., 2021. Individual EEG profiling of attention deficits in left spatial neglect: a pilot study. Neurosci. Lett. 761, 136097. doi:10.1016/j.neulet.2021.136097.

Lasaponara, S., D'Onofrio, M., Pinto, M., Dragone, A., Menicagli, D., Bueti, D., Lucia, M.D., Tomaiuolo, F., Doricchi, F., 2018. EEG correlates of preparatory orienting, contextual updating, and inhibition of sensory processing in left spatial neglect. J. Neurosci. 38, 3792–3808. doi:10.1523/JNEUROSCI.2817-17.2018.

Lasaponara, S., Pinto, M., Aiello, M., Tomaiuolo, F., Doricchi, F., 2019. The hemispheric distribution of α-band eeg activity during orienting of attention in patients with reduced awareness of the left side of space (Spatial neglect). J. Neurosci. 39, 4332–4343. doi:10.1523/JNEUROSCI.2206-18.2019.

Lee, H., Golkowski, D., Jordan, D., Berger, S., Ilg, R., Lee, J., Mashour, G.A., Lee, U.C., Avidan, M.S., Blain-Moraes, S., Golmirzaie, G., Hardie, R., Hogg, R., Janke, E., Kelz, M.B., Maier, K., Maybrier, H., McKinstry-Wu, A., Muench, M., Ochroch, A., Palanca, B.J.A., Picton, P., Schwarz, E.M., Tarnal, V., Vanini, G., Vlisides, P.E., 2019. Relationship of critical dynamics, functional connectivity, and states of consciousness in large-scale human brain networks. Neuroimage 188, 228–238. doi:10.1016/j.neuroimage.2018.12.011.

Makeig, S., Bell, A., Jung, T.P., Sejnowski, T., 1996. Independent component analysis of electroencephalographic data. In: Touretzky, D., Mozer, M.C., Hasselmo, M. (Eds.), Adv. Neural Inf. Process. Syst., Vol. 8. MIT Press, Cambridge, MA.

Mancuso, M., Damora, A., Abbruzzese, L., Navarrete, E., Basagni, B., Galardi, G., Caputo, M., Bartalini, B., Bartolo, M., Zucchella, C., Carboncini, M.C., Dei, S., Zoccolotti, P., Antonucci, G., De Tanti, A., 2019. A new standardization of the bells test: an Italian multi-center normative study. Front. Psychol. 9, 2745. doi:10.3389/fpsyg.2018.02745.

Moes, P.E., Brown, W.S., Minnema, M.T., 2007. Individual differences in interhemispheric transfer time (IHTT) as measured by event related potentials. Neuropsychologia 45, 2626–2630. doi:10.1016/j.neuropsychologia.2007.03.017.

Mort, D.J., Malhotra, P., Mannan, S.K., Rorden, C., Pambakian, A., Kennard, C., Husain, M., 2003. The anatomy of visual neglect. Brain 126, 1986–1997. doi:10.1093/brain/awg200.

Oliveri, M., 2011. Brain stimulation procedures for treatment of contralesional spatial neglect. Restor. Neurol. Neurosci. doi:10.3233/RNN-2011-0613.

Parkes, L., Tiego, J., Aquino, K., Braganza, L., Chamberlain, S.R., Fontenelle, L.F., Harrison, B.J., Lorenzetti, V., Paton, B., Razi, A., Fornito, A., Yücel, M., 2019. Transdiagnostic variations in impulsivity and compulsivity in obsessive-compulsive disorder and gambling disorder correlate with effective connectivity in cortical-striatal-thalamic-cortical circuits. Neuroimage 202, 116070. doi:10.1016/j.neuroimage.2019.116070.

Parr, T., Friston, K.J., 2018. The computational anatomy of visual neglect. Cereb. Cortex 28, 777–790. doi:10.1093/cercor/bhx316.

Parton, A., Malhotra, P., Husain, M., 2004. Hemispatial neglect. J. Neurol. Neurosurg. Psychiatry 75, 13–21.

Pellicciari, L., Piscitelli, D., Basagni, B., Tanti, A.D., Algeri, L., Caselli, S., Ciurli, M.P., Conforti, J., Estraneo, A., Moretta, P., Gambini, M.G., Inzaghi, M.G., Lamberti, G., Mancuso, M., Rinaldesi, M.L., Sozzi, M., Abbruzzese, L., Zettin, M., Porta, F.L., 2020. 'Less is more': validation with Rasch analysis of five short-forms for the Brain Injury Rehabilitation Trust Personality Questionnaires (BIRT-PQs). Brain Inj. 34, 1741–1755. doi:10.1080/02699052.2020.1836402.

Peylo, C., Hilla, Y., Sauseng, P., 2021. Cause or consequence? Alpha oscillations in visuospatial attention. Trends Neurosci. 44, 705–713. doi:10.1016/j.tins.2021.05.004.

Pietrelli, M., Zanon, M., Làdavas, E., Grasso, P.A., Romei, V., Bertini, C., 2019. Posterior brain lesions selectively alter alpha oscillatory activity and predict visual performance in hemianopic patients. Cortex 121, 347–361. doi:10.1016/j.cortex.2019.09.008.

Qureshi, A.A., Zhang, C., Zheng, R., Elmeligi, A., 2018. Ischemic stroke detection using EEG signals. In: Proceedings of the 28th Annual International Conference on Computer Science and Software Engineering, pp. 301–308.

Raykov, T., Marcoulides, G.A., 2006. Estimation of generalizability coefficients via a structural equation modeling approach to scale reliability evaluation. Int. J. Test. 6, 81–95. doi:10.1207/s15327574ijt0601_5.

Romei, V., Brodbeck, V., Michel, C., Amedi, A., Pascual-Leone, A., Thut, G., 2008. Spontaneous fluctuations in posterior α-band EEG activity reflect variability in excitability of human visual areas. Cereb. Cortex 18, 2010–2018. doi:10.1093/cercor/bhm229.

Romei, V., Chiappini, E., Hibbard, P.B., Avenanti, A., 2016. Empowering reentrant projections from V5 to V1 boosts sensitivity to motion. Curr. Biol. 26, 2155–2160. doi:10.1016/j.cub.2016.06.009.

Samaha, J., Postle, B.R., 2015. The speed of alpha-band oscillations predicts the temporal resolution of visual perception. Curr. Biol. 25, 2985–2990. doi:10.1016/j.cub.2015.10.007.The.

Shapiro, S.S., Wilk, M.B., 1965. An analysis of variance test for normality (Complete Samples). Biometrika 52, 591–611. doi:10.2307/2333709.

Stam, C.J., Nolte, G., Daffertshofer, A., 2007. Phase lag index: Assessment of functional connectivity from multi channel EEG and MEG with diminished bias from common sources. Hum. Brain Mapp. 28, 1178–1193. doi:10.1002/hbm.20346.

Tenenhaus, M., Vinzi, V.E., Chatelin, Y.M., Lauro, C., 2005. PLS path modeling. Comput. Stat. Data Anal. 48, 159–205. doi:10.1016/j.csda.2004.03.005, Partial Least Squares.

Thiebaut de Schotten, M., Dell'Acqua, F., Forkel, S., Simmons, A., Vergani, F., Murphy, D.G.M., Catani, M., 2011. A lateralized brain network for visuo-spatial attention. Nat. Preced. 1–1. doi:10.1038/npre.2011.5549.1.

Thut, G., Nietzel, A., Brandt, S., Pascual-Leone, A., 2006. Alpha band electroencephalographic activity over occipital cortex indexes visuospatial attention bias and predicts visual target detection. J. Neurosci. 13, 9494–9502. doi:10.1523/JNEUROSCI.0875-06.2006.

Trajkovic, J., Di Gregorio, F., Ferri, F., Marzi, C., Diciotti, S., Romei, V., 2021. Resting state alpha oscillatory activity is a valid and reliable marker of schizotypy. Sci. Rep. 11, 10379. doi:10.1038/s41598-021-89690-7.

Trajkovic, J., Di Gregorio, F., Marcantoni, E., Thut, G., Romei, V., 2022. A TMS/EEG protocol for the causal assessment of the functions of the oscillatory brain rhythms in perceptual and cognitive processes. STAR Protoc. 3, 101435. doi:10.1016/j.xpro.2022.101435.

Ungerleider, L., Haxby, J.V., 1994. What" and "where" in the human brain. Curr. Opin. Neurobiol. 4, 157–165. doi:10.1016/0959-4388(94)90066-3.

VanRullen, R., 2016. Perceptual cycles. Trends Cogn. Sci. 20, 723–735. doi:10.1016/j.tics.2016.07.006.

Verleger, R., Heide, W., Butt, C., Wascher, E., Kömpf, D., 1996. On-line brain potential correlates of right parietal patients' attentional deficit. Electroencephalogr. Clin. Neurophysiol. 99, 444–457. doi:10.1016/S0013-4694(96)95645-X.

Vinck, M., Oostenveld, R., Van Wingerden, M., Battaglia, F., Pennartz, C.M.A., 2011. An improved index of phase-synchronization for electrophysiological data in the presence of volume-conduction, noise and sample-size bias. Neuroimage 55, 1548–1565. doi:10.1016/j.neuroimage.2011.01.055.

Vinzi, V.E., Trinchera, L., Amato, S., 2010. PLS path modeling: from foundations to recent developments and open issues for model assessment and improvement. In: Esposito Vinzi, V., Chin, W.W., Henseler, J., Wang, H. (Eds.), Handbook of Partial Least Squares: Concepts, Methods and Applications, Springer Handbooks of Computational Statistics. Springer, Berlin, Heidelberg, pp. 47–82. doi:10.1007/978-3-540-32827-8_3.

Wang, X., Xu, X., Han, H., He, R., Zhou, L., Liang, R., Yu, H., 2019. Using structural equation modeling to detect response shift in quality of life in patients with Alzheimer's disease. Int. Psychogeriatr. 31, 123–132. doi:10.1017/S1041610218000595.

Wutz, A., Melcher, D., Samaha, J., 2018. Frequency modulation of neural oscillations according to visual task demands. Proc. Natl. Acad. Sci. USA 115, 1346–1351. doi:10.1073/pnas.1713318115.

Xia, Y., Yang, Y., 2019. RMSEA, CFI, and TLI in structural equation modeling with ordered categorical data: the story they tell depends on the estimation methods. Behav. Res. 51, 409–428. doi:10.3758/s13428-018-1055-2.

Zazio, A., Schreiber, M., Miniussi, C., Bortoletto, M., 2020. Modelling the effects of ongoing alpha activity on visual perception: the oscillation-based probability of response. Neurosci. Biobehav. Rev. 112, 242–253. doi:10.1016/j.neubiorev.2020.01.037.